Neutron reflectivity study of end-adsorbed diblock copolymers : cross-over from nushrooms to brushes

John Field, C. Toprakcioglu, L. Dai, G. Hadziioannou, G. Smith, W. Hamilton

Classification
Physics Abstracts
61.12E — 61.40K — 68.45 — 68.60

Neutron reflectivity study of end-adsorbed diblock copolymers : cross-over from mushrooms to brushes

J. B. Field ([1]), C. Toprakcioglu ([1]), L. Dai ([1]), G. Hadziioannou ([2]), G. Smith ([3]) and W. Hamilton ([3])

([1]) Cavendish Laboratory, Madingley Road, Cambridge CB3 0HE, Great-Britain
([2]) Department of Polymer Chemistry, University of Groningen, 9747 AG Groningen, The Netherlands
([3]) LANSCE, Los Alamos National Laboratory, Los Alamos, New Mexico 87545, U.S.A.

(*Received 7 July 1992, accepted 7 September 1992*)

Abstract. — We report neutron reflectivity data on polystyrene-poly(vinyl-2-pyridine) (PS-PVP) diblock copolymers adsorbed onto quartz from the selective solvent toluene (a good solvent for PS, but a poor one for PVP). The PVP « anchor » block adsorbs strongly to form a thin layer on the quartz substrate, while the PS chains dangle into the solvent. The grafting density of the non-adsorbing PS chains is varied by varying the size of the PVP block, while the PS molecular weight is kept constant. The PS adsorbance decreases systematically with increasing PVP molecular weight. The form of the polymer density profile normal to the substrate is found to change with the PS grafting density, and a transition from a « brush » to a « mushroom » conformation is observed as the PVP molecular weight is increased. For the copolymers with a high PVP content, the dependence of the maximum in the polymer density profile on the mean distance, s, between anchor points obeys the scaling law expected of mushrooms, while s increases with increasing molecular weight of the anchor block also in a manner consistent with a mushroom model.

Introduction.

The adsorption of polymers at the solid-liquid interface is known to play an important role in the steric stabilization of colloidal dispersions and other technologically important applications such as adhesion and lubrication. The use of diblock copolymers is particularly interesting in this connection, as under suitable conditions these macromolecules are capable of adsorbing *via* one block, while the other, non-adsorbing block stretches away from the surface into solution. When two surfaces covered with end-adsorbed diblock copolymer chains approach, long-range repulsive steric forces emerge as the stretched chains overlap, while there is no possibility of any attractive bridging forces which are often seen in homopolymer systems at low surface coverage. The strength of adsorption and the extent of stretching of such diblock chains, however, depend both on the composition and molecular weight of each polymeric block as well as the solvent quality. The conformation of adsorbed diblock chains is therefore

expected to be sensitive to these parameters. Clearly, knowledge of the chain conformations in adsorbed layers is essential for a detailed understanding of a wide range of interfacial phenomena at the molecular level.

Recently, the technique of neutron reflectometry has been shown to provide good resolution for the determination of polymer density profiles [1-5]. Small-angle neutron scattering has also been used in the study of end-attached polymer layers [6, 7], although this technique is less sensitive to the detailed features of the polymer density profile. The adsorption of end-attached, protonated polystyrene-polyethyleneoxide (PS-PEO) diblock copolymer from deuterated toluene (a good solvent) onto quartz has already been investigated using neutron reflectrometry [5]. The PEO block, which comprised a small fraction of the total molecular weight, strongly adsorbed on the quartz substrate, while the PS block remained in solution forming a semidilute stretched polymer « brush ». The reflectivity profiles in this study were well-described by a parabolic or error function polymer density profile normal to the interface between the quartz and the solvent, in agreement with mean field calculations [8, 9], numerical calculations [1] based on the Scheutjens and Fleer self consistent field method [10-12] and Monte Carlo simulations [13, 1, 14]. The layer thickness values were found to be in good agreement with results of interlayer force measurements for the same polymer-solvent system adsorbing onto mica [15]. The molecular weight dependence of the layer thickness and adsorbance was also found to obey scaling laws in accord with the scaling [16, 17] and mean field theories [8, 9] of semidilute polymer brushes.

For end-grafted chains, scaling arguments have been used to distinguish between two regimes, « mushrooms » or « brushes » depending on the surface coverage [16, 17]. The two different regimes may be characterized by the mean distance, s, between anchor points, and the polymer density profile which defines the thickness, L_0, of the adsorbed layer. At high surface coverage, brushes are formed, s is small compared to the Flory radius, R_F, of the non-adsorbing chains and the extension ratio, L_0/s, is high. For mushrooms, however, the extension ratio is expected to be ~ 1 and the distance between anchor points is greater than R_F.

The surface coverage of adsorbed chains depends on their adsorption energy. In general, the « sticking energy » of a diblock chain is determined by the nature and size of the adsorbing group, A. The ratio of the polymerization indices N_A and N_B of the two blocks is an important parameter. For large N_B/N_A, the adsorbance, Γ_B, of the B-block is expected to increase with increasing N_A (i.e. as the sticking energy is increased). For low N_B/N_A, however, Γ_B is expected to decrease with increasing N_A as the distance between anchor points, s, becomes controlled by the area occupied by the adsorbing blocks on the surface. The ratio, N_B/N_A, therefore determines whether the polymer configuration is a brush or a mushroom. By varying N_A, while keeping N_B fixed, it is possible to change the structure of the adsorbed layer from that of a brush (low N_A) to that of a mushroom (high N_A). While in our previous investigation [5] we studied adsorbed layers of highly asymmetric PS-PEO block copolymers which form only polymer brushes, in the present paper we report results of neutron reflectivity on diblock copolymers of protonated polystyrene-poly(vinyl-2-pyridine) (PS-PVP) terminally adsorbed on quartz from deuterated toluene *via* the PVP block whose size, in this case, is comparable to that of the PS. Here the PS block size, N_B, is kept constant and the density profile investigated for different PVP block sizes, N_A.

Experimental.

The experimental set up is the same as that described in a previous paper [5]. The neutron beam is passed through an optically flat quartz slab and reflected off its lower surface which is immersed in a reservoir of polymer solution contained in a Teflon cell [5]. The results reported

in the present study were obtained on SPEAR at Los Alamos, and D17 at the ILL Grenoble. SPEAR uses a fixed angle of incidence with a pulsed neutron beam and time-of-flight (TOF) to measure the wavelength [3, 4]. A wavelength range of 0.5 to 16 Å and a glancing angle of incidence of 0.45° were used here. D17 uses a monochromatic neutron beam whose angle of incidence was varied by rotating the sample to give the required Q-range. Here wavelengths of 12 Å, 20 Å and 30 Å, and an angular range of 0.7° to 1.825° were used. The Q-ranges used allowed the critical edge to be measured on both instruments. The deuterated solvents were purchased from MSD Isotopes. The synthesis and characterisation of the PS-PVP block copolymers has been previously described [18] (see Tab. I). All materials were used as supplied.

Table I. — *Table of* PS-PVP *diblock copolymer samples of* PS *molecular weight,* PS M_W, *and* PVP *molecular weight,* PVP M_W. *The polydispersity,* M_W/M_N, *of both blocks is approximately* 1.1.

PS M_W	PVP M_W
60×10^3	5×10^3
60×10^3	30×10^3
60×10^3	60×10^3
60×10^3	120×10^3

It is important to ensure that the substrate on which the polymer molecules adsorb is clean. Before each measurement the quartz was cleaned in a mixture of 3 : 1 H_2SO_4 . HNO_3 followed by a mixture of 3 : 1 HCl : HNO_3 both for ca. 4-6 hours. It was then washed thoroughly with distilled water, then with absolute alcohol, and dried in an oven. All glass components coming in contact with the solvent or the polymer solution were cleaned in chromic acid and then thoroughly washed in distilled water. Polymer solutions of 0.05 mg ml^{-1} were used, and adsorption was allowed to occur at room temperature, usually overnight.

Results and discussion.

Toluene is a poor solvent for PVP, but a good solvent for PS so that PS-PVP block copolymers are expected to form micelles above the critical micelle concentration (cmc). Using a mean field model, Munch and Gast [19] found that a critical adsorption concentration exists, analogous to the cmc in micellization. This was also found by Marques and Joanny [18] where in extremely dilute solutions, a threshold for adsorption was found to depend on the spreading power of the sticking group and on the strength of the sticking energy. This critical adsorption concentration (cac) was found to decrease as the surface attraction increases, as the copolymer-solvent compatibility decreases and as the more soluble block length decreases. In selective solvents the incompatibility is governed by the adsorbing block which is in poor solvent conditions, the non-adsorbing block being in good solvent conditions. Munch and Gast found that either adsorption or micellization occurred depending on the surface attraction and the incompatibility provided that the concentration is above the cac and the cmc respectively. In the adsorption region, the lower free energy of the adsorbed layer precludes the formation of micelles. When the overall concentration is below the cac in this region neither adsorption nor micellization occurs. Similarly, in the region of micellization, the free energy of micellization is lower than that of adsorption, preventing the formation of an adsorbed layer. The line

separating the two regions designates the boundary where the free energy of micelles equals that of adsorbed layers and the cac equals the cmc.

Well above both the cac and cmc, the adsorbed layer may be in equilibrium with the micellar solution [20]. Marques and Joanny found two adsorption regimes in equilibrium with the micellar solution depending on the asymmetry of the block copolymer. Essentially, they found mushrooms if the size of the solvated group was of the same order as that of the anchor group, and brushes if the solvated group was large compared to the anchor group. The size of the adsorbing block (PVP), for which the solvent (toluene) is a very poor one, in the present case, also affects the value of the cmc. While the block copolymers used in our study having a low PVP content micellise at concentrations above those we have used during adsorption, the possibility exists that the high-PVP content material (60-120) may be above its cmc in toluene. Nevertheless, it is known that PS does not adsorb onto quartz from toluene so it is difficult to imagine the PS-PVP diblock copolymers adsorbing in the form of micelles since the structure of micelles is that of « furry balls » with the PS shielding the PVP. The formation of micelles in solution is therefore not expected to affect the configuration of the chains on the surface, but may affect the adsorption kinetics since the micelles may have to open out and expose the PVP before the chains may stick, assuming that adsorption is favoured above micellization. Micellization of block copolymers has been shown by Internal Reflection Interferometry to dramatically affect their adsorption kinetics for this reason [21, 22].

According to de Gennes [23], in the mushroom regime each chain may be thought of as occupying roughly a half sphere with a radius comparable to the Flory radius for a polymer coil in a good solvent. Consider the interval $a \ll z \ll R_F$, where z is the distance perpendicular to the grafting plane and a is the monomer size. At $z \sim R_F$ it is expected that the concentration of monomers is equal to the concentration inside a single coil (N/R_F^3) times the fraction of wall area occupied by polymer coils $(\sigma/a^2)\,R_F^2$ where σ is the fraction of grafted points. Thus the concentration at a distance z, $\phi(z)$, is given by :

$$\phi(z = R_F) \sim N\sigma a/R_F = \sigma N^{2/5} \tag{1}$$

At the lower limit $(z \sim a)$, $\phi(z)$ should be equal to the fraction of grafted points, σ, where $\sigma = a^2/s^2$ and s is the distance between grafting points. Interpolating between these two ends by a power law gives :

$$\phi(z) = \sigma\,(z/a)^m \tag{2}$$

where m is an unknown exponent. Imposing the condition at $z = R_F$ gives :

$$\sigma\,(R_F/a)^m = \sigma N^{2/5} \quad \text{and} \quad m = 2/3\,. \tag{3}$$

For $z > R_F$ the concentration profile drops out very fast. If on the other hand, $s < R_F$, the polymer coils start to overlap forming stretched brushes. In this regime the density profile, $\phi(z)$, is expected to be flat and proportional to $s^{-4/3}$.

The method of analysis of reflectivity data has already been discussed in a previous paper in which the data could be fitted to a polymer brush-like density profile [5]. In view of the density profile predicted by de Gennes in equation (2), mushroom-like profiles were tried to fit the reflectivity data here, rather than the brush-like profiles used before [5], since in the study presented here the size of the adsorbing block, N_A, is varied. Mushroom-like profiles were constructed in two ways.

The first profile was constructed using a function similar to the Schultz function, namely :

$$\phi(z) = Az^n \exp(-\alpha z^\beta) \tag{4}$$

where for a Schultz function $\beta = 1$. The position of the maximum at $z = z_0$ when $\phi(z) = \phi_0 = \sigma N^{2/5}$ is given by $z_0 = (n/\beta\alpha)^{1/\beta}$ where $\phi_0 = A(n/\beta\alpha)^{1/\beta} \exp(-n/\beta)$. The second profile was constructed by sticking together two Gaussians of the form :

$$\phi(z) = \phi_0 \frac{\exp[-(z - z_0)^2/2\,\delta_i^2] - \exp[-(1/2\,\eta_i^2)]}{1 - \exp[-1/2\,\eta_i^2]} \tag{5}$$

of different widths δ_1 and δ_2 centred at z_0, where $z_0 = \delta/\eta_1$. The parameter, η_i, allows the density profile to shift parallel to the $\phi(z)$-axis. This allows some of the tail of the Gaussian to be removed so the profile can look very much like the Schultz function.

Using a density profile defined by equation (4), with $n = 2/3$, it was found that in order to fit the reflectivity data at high Q a layer of thickness ~ 15 Å and scattering length density close to that of PVP had to be introduced at the surface of the quartz. This relatively large surface layer of PVP compared to that of water, which was found at the quartz/toluene interface previously [5], dominates the reflectivity at high Q so a single layer of PVP was assumed in the model. The model scattering length density profile used to fit the reflectivity data to a function of the form defined by equation (4) is shown schematically in figure 1a. Fitting the reflectivity data to such a function, it was found that in order for the concentration profile to drop out fast enough for $z > R_F$, β had to be set equal to 2 to give the best fits. So, for fixed n and β, A is a function of α and ϕ_0, while α is a function z_0. In this way the number of fitting parameters is reduced to two. The reflectivity data was fitted allowing the parameters ϕ_0 and z_0 to vary. The fitted parameters for the three copolymers with the largest PVP anchor groups measured on SPEAR and D17 are shown in table II.

We note, however, that in the context of this model ϕ_0 and z_0 cannot vary independently, but are correlated (i.e. if z_0 is changed, this changes ϕ_0). For this reason this model density profile is not an ideal function to fit to, as it is preferable to vary the parameters independently. A skew Gaussian profile defined by equation (5) was therefore also used to try and fit the reflectivity data. This function has three fitting parameters but has the advantage that these parameters may vary independently and is thus more flexible than the Schultz function profile. It was found that the best fits were obtained for $\eta_1 = 2$ and $\eta_2 = 1/4$ so $\phi_1(z = z_0) = \phi_0$, $\phi_2(z = z_0) = \phi_0$, $\phi_1(z = 0) = 0$, and $\phi_2(z = 4\,\delta_2 - z_0) = 0$. Again a 15 Å layer of PVP was assumed in the model. The model scattering length density profile used to fit the reflectivity data to a function of this form is shown schematically in figure 1b. The fitted parameters for the three copolymers with the largest PVP anchor groups measured on SPEAR and D17 are shown in table III.

The block copolymer with 5×10^3 PVP M_W was measured on D17. The reflectivity data for this molecular weight could not be fitted to either of the above density profiles defined by equations (4) and (5). Good fits were obtained, however, with the brush-type density profiles used previously [5]. The fitted parameters for this molecular weight are shown in tables IVa and IVb.

These profiles are defined by the following equations :

$$\phi(z) = \phi_0 \left[1 - \left(\frac{z}{L_0}\right)^n\right] \tag{6}$$

and

$$\phi(z) = \frac{\phi_0}{2}\,(1 - \text{erf}\,((z - L_0)/(2\,\delta z)))\,. \tag{7}$$

The value of n in the polynomial profile defined by equation (6) determines the shape of the profile. It is 1 for a linear profile, 2 for a parabolic profile, and tends to infinity in the case of a

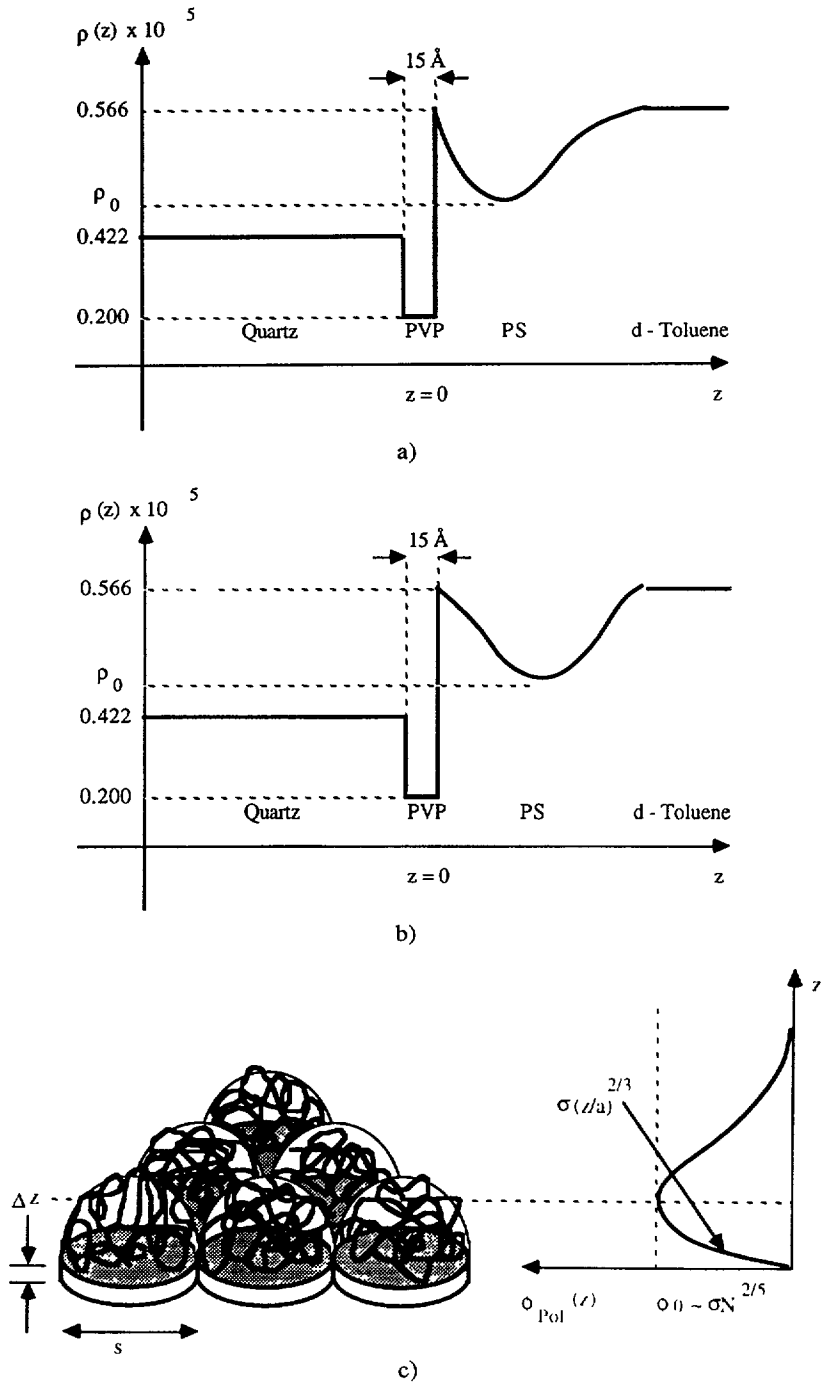

Fig. 1. — a) Model scattering length density profile, $\rho(z) \times 10^{-5}$ Å^{-2}, used to fit the reflectivity data to a Schultz function defined by equation (4). b) Model scattering length density profile, $\rho(z) \times 10^{-5}$ Å^{-2}, used to fit the reflectivity data to a skew Gaussian function defined by equation (5). c) Schematic diagram representing PS-PVP block copolymer chains adsorbed at the solid-liquid interface from a selective solvent. The PVP forms a monolayer spread out in « pancakes » on the surface and the PS forms « mushrooms ». The corresponding polymer density profile is also shown schematically.

Table II. — *Parameters obtained from fits to the Schultz function density profile defined by equation* (4) *for the* PS-PVP *data measured on* SPEAR *and* D17. Γ_A *is the* PVP *adsorbance and* Γ_B *is the* PS *adsorbance. The* M_W *of the* PS *block is* 60×10^3 *in each case (see* Tab. I).

PVP M_W	Instrument	z_0 (Å)	ϕ_0 (%)	Γ_A (mg m^{-2})	Γ_B (mg m^{-2})	s (Å)
30×10^3	SPEAR	100 ± 10	9.3 ± 0.2	0.9 ± 0.2	1.7 ± 0.3	75 ± 5
30×10^3	D17	80 ± 10	8.0 ± 0.2	0.8 ± 0.2	1.6 ± 0.3	80 ± 5
60×10^3	SPEAR	90 ± 10	3.8 ± 0.2	0.7 ± 0.1	0.7 ± 0.1	120 ± 10
120×10^3	SPEAR	90 ± 10	2.8 ± 0.2	1.0 ± 0.2	0.5 ± 0.1	140 ± 10

Table III. — *Parameters obtained from fits to the skew Gaussian density profile defined by equation* (5) *for the* PS-PVP *data measured on* SPEAR *and* D17. Γ_A *is the* PVP *adsorbance and* Γ_B *is the* PS *adsorbance. The* M_W *of the* PS *block is* 60×10^3 *in each case* (see Tab. I).

PVP M_W	Instrument	z_0 (Å)	ϕ_0 (%)	δ_2 (Å)	Γ_A (mg m^{-2})	Γ_B (mg m^{-2})	s (Å)
30×10^3	SPEAR	90 ± 10	9.3 ± 0.2	90 ± 10	0.8 ± 0.2	1.5 ± 0.3	80 ± 5
30×10^3	D17	100 ± 10	7.3 ± 0.2	70 ± 10	0.7 ± 0.2	1.4 ± 0.3	85 ± 5
60×10^3	SPEAR	90 ± 10	3.9 ± 0.2	90 ± 10	0.7 ± 0.1	0.7 ± 0.1	120 ± 10
120×10^3	SPEAR	140 ± 10	2.8 ± 0.2	40 ± 10	0.8 ± 0.2	0.4 ± 0.1	160 ± 10

Table IV. — a) *Parameters obtained from fits to the parabolic density profile defined by equation* (6) *for the* PS-PVP *copolymer with a* PVP M_W *of* 5×10^3. Γ_A *is the* PVP *adsorbance and* Γ_B *is the* PS *adsorbance.* b) *Parameters obtained from fits to the error-function density profile defined by equation* (7) *for the* PS-PVP *copolymer with a* PVP M_W *of* 5×10^3. Γ_A *is the* PVP *adsorbance and* Γ_B *is the* PS *adsorbance.*

a)

PVP M_W	L_0 (Å)	n	ϕ_0 (%)	Γ_A (mg m^{-2})	Γ_B (mg m^{-2})	s (Å)
5×10^3	320 ± 30	3.6 ± 0.5	9.0 ± 0.2	0.2 ± 0.03	2.3 ± 0.4	65 ± 5

b)

PVP M_W	L_0 (Å)	δ (Å)	ϕ_0 (%)	Γ_A (mg m^{-2})	Γ_B (mg m^{-2})	s (Å)
5×10^3	260 ± 20	80 ± 10	9.0 ± 0.2	0.2 ± 0.03	2.3 ± 0.4	65 ± 5

step function. For $0 < n < 1$ the profile becomes concave upwards. The parameter ϕ_0 defines the volume fraction of polymer at the quartz/d-toluene interface and L_0 defines the thickness of the adsorbed layer where $\phi(L_0) = 0$. The error function profile defined by equation (7) has the properties that erf $(0) = 0$, erf $(+\infty) = 1$ and erf $(-\infty) = -1$ where δz is the roughness of the layer.

The fitted parameters for the three highest PVP M_W show that the volume fraction of polymer at the maximum in the density profile, ϕ_0, and the PS coverage, Γ_B, decrease with

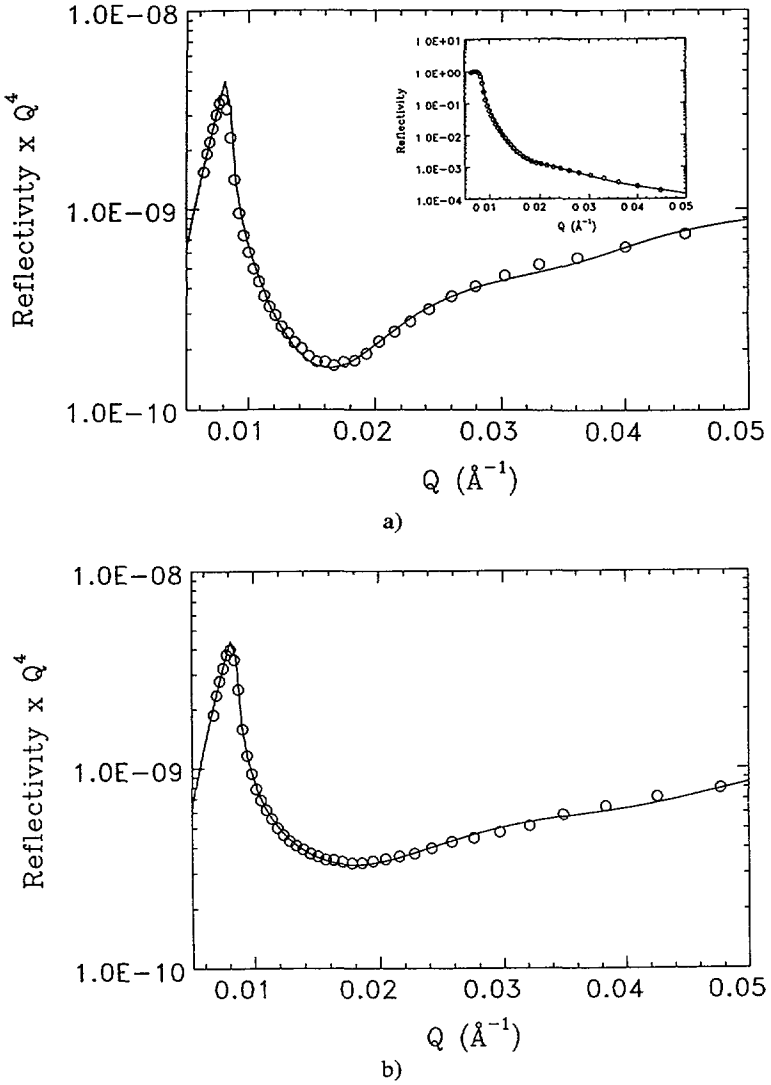

Fig. 2. — a) Reflectivity $\times Q^4$ of PVP $M_W = 30 \times 10^3$ block copolymer measured on SPEAR (O) and fit based on the Schultz function model defined by equation (4). The fitted parameters used here are shown in table II. The inset shows the same data and best fit in the form of Reflectivity *vs.* Q. b) Reflectivity $\times Q^4$ of PVP $M_W = 60 \times 10^3$ block copolymer measured on SPEAR (O) and fit based on the Schultz function model defined by equation (4). The fitted parameters used here are shown in table II. c) Reflectivity $\times Q^4$ of PVP $M_W = 120 \times 10^3$ block copolymer measured on SPEAR (O) and fit based on the Schultz function model defined by equation (4). The fitted parameters used here are shown in table II.

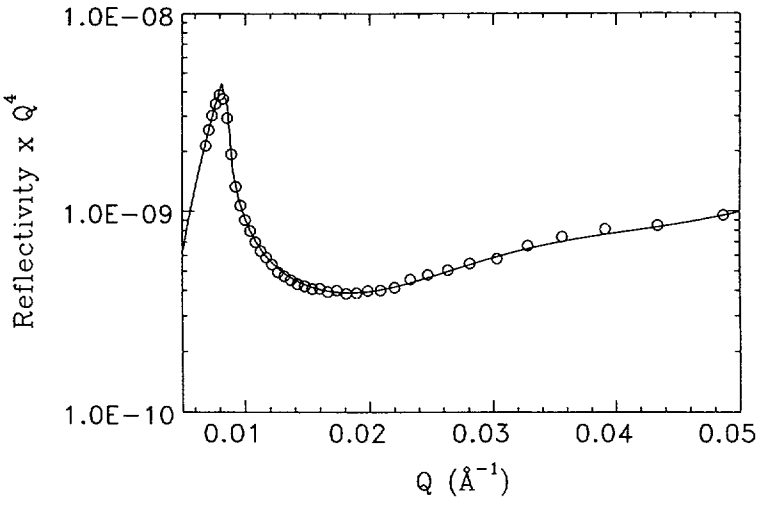

c)

Fig. 2 *(continued).*

increasing PVP M_W and the distance between anchor groups, s, increases with increasing PVP M_W whilst the thickness of the layer stays relatively constant. These trends are indicative of mushrooms. The lowest PVP M_W however shows trends more consistent with brushes.

The reflectivity fits for the three highest PVP molecular weights are shown in figure 2 based on the fitted parameters given in table II and the density profiles are shown in figure 3 for the two different functions based on the fitted parameters given in tables II and III. As can be seen from the reflectivity plots the fits are rather good. It should be noted, however, that it is easier to get « good fits » to reflectivity data with only a few features than to data which, for example, exhibit a series of fringes. The Schultz function and Gaussian density profiles for the 30×10^3 and 60×10^3 PVP molecular weights are almost identical in shape. There is some discrepancy between the two density profiles for the highest PVP molecular weight but this can

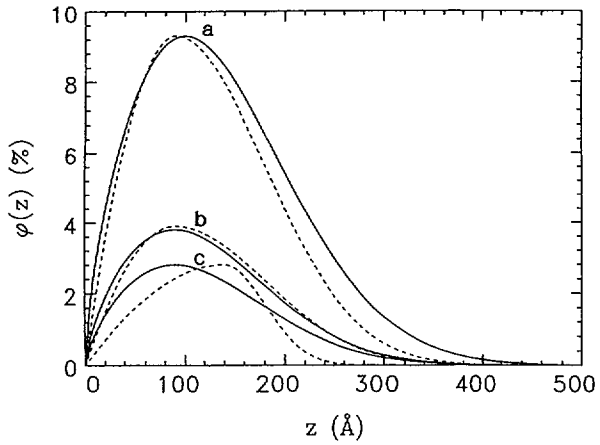

Fig. 3. — Schultz function (——) and skew Gaussian (------) polymer volume fraction profiles $\phi(z)$, for a) 30×10^3 PVP M_W, b) 60×10^3 PVP M_W and c) 120×10^3 PVP M_W measured on SPEAR. The fitted parameters used here are shown in tables II and III.

be attributed to the low contrast between the adsorbed layer and the solvent, thus rendering the fit less sensitive to the density profile as observed before with the PS-PEO samples at low coverage [5]. These three molecular weights could not be fitted to a parabolic profile or a brush-like profile with a depletion layer. This data could also not be fitted to a 2-sublayer or 3-sublayer model with or without roughness between the sublayers. The fitted density profiles defined by the two different functions (i.e. polynomial and error function respectively) for the lowest PVP M_W measured on D17 based on the fitted parameters given in tables IVa and IVb are shown in figure 4. The value of the exponent, n, is higher than 2 for this molecular weight, although from the fitting it is clearly in the brush regime showing no depletion layer at the surface. Both the functions fitted to this data give broadly the same overall shape of density profile (see Fig. 4).

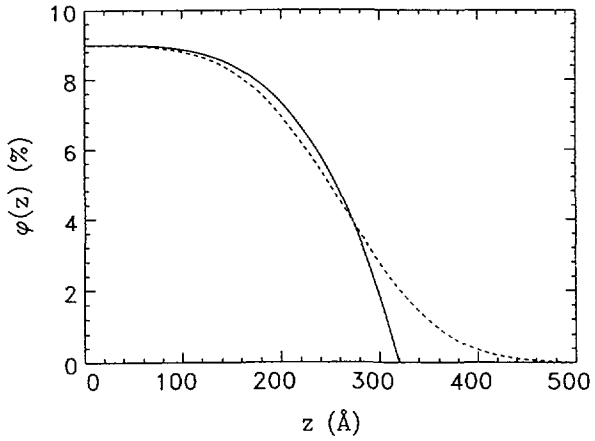

Fig. 4. — Polynomial (——) and error function (------) polymer volume fraction profiles, $\phi(z)$, defined by equations (6) and (7) for the lowest PVP $M_W = 5 \times 10^3$ measured on SPEAR. The fitted parameters used here are shown in tables IVa and IVb.

The lowest molecular weight PVP sample which has a PVP M_W of 5×10^3 and a PS M_W of 60×10^3 is consistent with the data obtained from the highly asymmetric PS-PEO block copolymers previously [5] in that it gives a brush with a smaller layer thickness and distance between anchor groups than the PS-PEO with the lowest M_W (80×10^3) investigated in that study, although the exponent, n, is somewhat greater than 2. A greater exponent is however expected at higher surface densities [24]. The higher exponent may therefore reflect a more compact brush due to the different anchor group. The layer thickness obtained with this PVP sample in the present study is also in reasonable agreement with that determined by surface force measurements for a PS-PEO copolymer of similar M_W [15].

As can be seen the fitted parameters and the density profiles of both model functions (i.e. modified Schultz function and skew Gaussian respectively) for the three highest molecular weights are consistent with a mushroom conformation of the chains and not with a brush conformation. The thickness of the adsorbed layer remains essentially constant with changing PVP size, and the mean distance between anchor points increases with increasing PVP size which is accompanied by a decrease in the PS adsorbance. It is valid here to think of the density profile being averaged over the surface since the coherence length of neutrons is much greater than the distance between anchor groups. Figure 5 shows a plot of log (ϕ_0) against log s and gives a straight line of gradient close to -2.0. In the mushroom regime, for fixed N_B, it is predicted that $\phi_0 \sim s^{-2}$ [21] (see Eq. (1)) which is confirmed by the data.

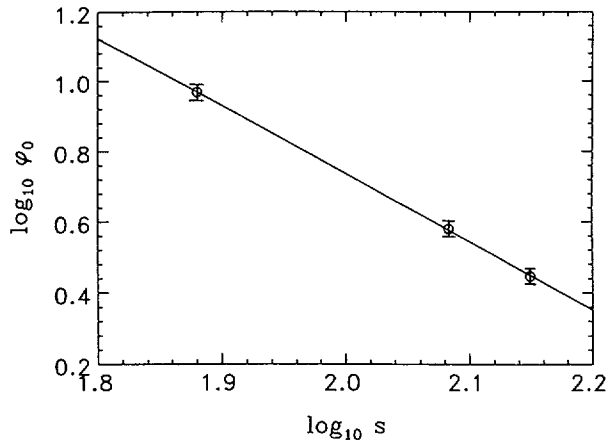

Fig. 5. — A plot of $\log_{10} \phi_0$ *vs.* $\log_{10} s$ for PS-PVP polymers measured on SPEAR showing a gradient of -1.9 ± 0.1.

The adsorbance of PS-PVP block copolymers with a wide range of molecular weights was studied by Parsonage *et al.* [25] using scintillation counting from tritium labelled copolymers, and X-ray photoemission spectroscopy. Only two of our copolymers (with PVP M_W of 60×10^3 and 120×10^3) have comparable molecular weights to the corresponding materials used by these authors. The adsorbance values obtained from our data for these two copolymers (see Tabs. II and III) are in reasonable agreement with those reported by Parsonage *et al.* [25].

The PVP block may be thought of as forming a thin layer spread out in a « pancake » on the surface, each block being confined inside a disc of diameter, s, and thickness Δz. This schematic picture is shown in figure 1c. The volume of the disc is proportional to s^2 if Δz is assumed to be constant which appears to be the case from the fits. So the number of monomers in the PVP block, N_A, or the PVP M_W, is proportional to s^2. Figure 6 shows a plot of log PVP M_W *vs.* log s. As can be seen, the data can be fitted to a straight line of gradient close to 2.0 as predicted by this simple model. From the mean distance between anchor groups, s, the volume fraction of polymer in the PVP layer is calculated to be ca. 0.75 which is consistent with this model, so in this picture the anchor block avoids the poor solvent and optimizes its

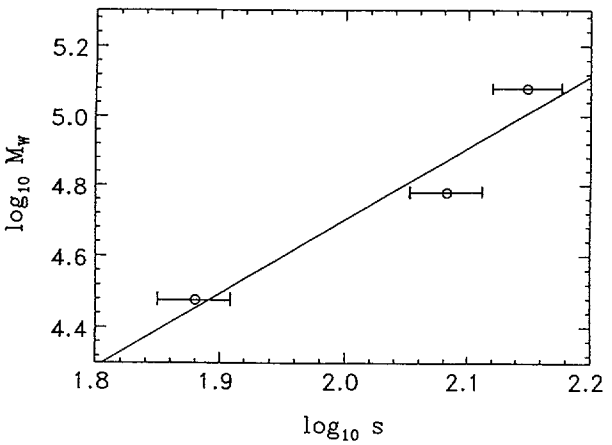

Fig. 6. — A plot of $\log_{10} s$ *vs.* $\log_{10} M_W$ for PS-PVP polymers, where M_W is the molecular weight of the PVP block. The straight line is a least-squares fit with a gradient of 2.2 ± 0.3.

contact with the substrate by spreading out on the surface rather than remaining as a dense coil. This result is in reasonable accord with the phase diagram determination of Parsonage *et al.* on the PVP/toluene system [25]. These authors report that for high molecular weights of the PVP block ($> 30 \times 10^3$), the PVP precipitates out of solution and the PVP-rich phase contains up to about 50 % toluene.

The extension ratio is between 0 and 2 if the layer thickness is defined as the position of the maximum in the density profile or between 1.5 and 2.5 for the skew Gaussian profile if the thickness is defined as $z_0 + \delta_2$ where z_0 is the centre of the skew Gaussian and δ_2 is the width of the right-hand Gaussian. The latter is perhaps a more realistic measure of the thickness since clearly the area under the profile, up to some thickness, must contain the majority of polymer. The distance between anchor points is somewhat greater than, but comparable to R_F so the mushrooms cannot be thought of as being separate but rather as slightly overlapping. The PS-PVP results for the three highest M_W polymers are consistent with the scaling predictions for mushrooms and although there is some overlap between the chains, the latter are not extended significantly. The conformation of the polymers may therefore be thought of as lying somewhere in the crossover between brushes and mushrooms. Thus, at fixed N_B the transition from brushes to mushrooms is driven by the increasing molecular weight of the adsorbing A block which controls the grafting density of the block copolymers. A similar « pancake » to brush transition in the case of copolymers in which both blocks can adsorb to the surface has recently been reported by Ou-Yang and Gao [26], who used dynamic light scattering to measure the hydrodynamic thickness of the polymer layers adsorbed on polystyrene latex particles. In his case too, the transition appears to be driven by the grafting density which was controlled by varying the bulk concentration of polymer. The mushroom to brush transition was also observed in the adsorption kinetics of asymmetric PS-PEO block copolymers [27], where in the early stages of adsorption a diffusion-controlled process is observed which is characteristic of mushrooms. As the surface coverage increases with time, the mushrooms begin to overlap and the cross-over to a brush regime is indicated by a slowing down of the adsorption process during later stages [27].

The adsorption of the PS-PVP as micelles leading to structures such as hemi-micelles on the surface has not been considered here. The consistency of the results with the proposed mushroom model, however, suggests that the PS-PVP copolymer chains are not adsorbing as micelles. If the PS-PVP chains were adsorbing as micelles, a more « brushy » conformation would be expected. A thicker adsorbed layer would be observed in such a case since the chains in the micelle would be expected to be stretched.

Monte Carlo simulations of the configurational properties of adsorbed chains reveal a crossover from essentially unperturbed chains at low surface coverage to strongly stretched chains at high surface coverage [13]. The effect of chain composition on the adsorbed amount and layer thickness has been studied by Evers *et al.* using the Self Consistent Field (SCF) theory of Scheutjens and Fleer [28]. They found that the adsorbed amound and layer thickness of adsorbed block copolymers depend strongly on the chain composition. When the total length of the diblock copolymer is kept constant, they found a maximum in the total coverage, Γ, as a function of the fraction of adsorbing segments. This maximum was found at a lower fraction of adsorbing segments with increasing chain length, bulk solution concentration and surface affinity of the anchor group.

It may be assumed that the total sticking energy of a chain is proportional to the number of sticking monomers, n, where the fraction of sticking monomers, f, is equal to n/N_A. Then assuming an equilibrium picture, balancing the total sticking energy to the repulsive energy gives, for a brush :

$$\frac{N_B}{g} k_B T = \varepsilon f N_A k_B T \tag{8}$$

where g is the number of monomers in each « blob » in the Alexander model [16] (i.e. $s \sim g^{3/5}$), and ε is the sticking energy (in $k_B T$ units) per adsorbing monomer. It follows that :

$$s \sim \left(\frac{N_B}{f N_A} \right)^{3/5} \tag{9}$$

but, since $\Gamma_B \sim \sigma N_B = N_B s^{-2}$, we obtain :

$$\Gamma_B \sim N_B^{-1/5} N_A^{6/5} f^{6/5} \tag{10}$$

For sufficiently large N_A, the fraction f approaches some constant value less than 1, so that $\Gamma_B \sim N_A^{6/5}$ at fixed N_B in the *brush* regime. (For very small values of N_A, f is expected to be a decreasing function of N_A, so that the variation of Γ_B with N_A may be somewhat slower than that suggested by a 6/5 exponent). On the other hand, using the simple model for *mushrooms* suggested by our data, $\Gamma_B \sim N_A^{-1}$. We thus have two opposing modes of behaviour as shown in figure 7

$$\Gamma_B \sim N_A^{6/5} \text{ (brush)} \quad \text{and} \quad \Gamma_B \sim N_A^{-1} \text{ (mushrooms)} . \tag{11}$$

Since brushes occur at low N_A and mushrooms at high N_A, provided N_B is kept fixed in each case, it follows that there is a maximum in the adsorbance Γ_B (see Fig. 7).

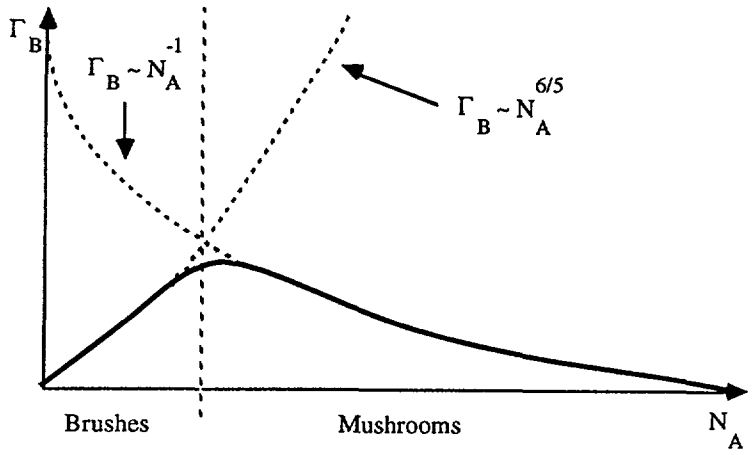

Fig. 7. — Plot of the adsorbance of the B block, Γ_B, as a function of size of anchor block, N_A. The plot shows a transition from brushes to mushrooms as the size of the anchor block is increased.

Conclusions.

The results of these and previous neutron reflectivity experiments confirm that two regimes of end-adsorbed block copolymers exist depending on the grafting density, and that the grafting density may be varied by varying the size of the anchor block. These regimes are characterized by two distinctly different density profiles which are distinguishable using neutron reflectometry. The PS-PVP block copolymers, in which the size of the non-adsorbing block (PS) is fixed, adsorb either forming a stretched polymer brush or a mushroom depending on the size of the anchor block (PVP). The polymer density profile normal to the substrate for the larger anchor blocks is well - described by the mushroom - type profile predicted by scaling theories in which

the polymer chains are not stretched, forming independent or weakly-interacting hemispheres on the surface. It is found that for polymers in the mushroom regime, the layer thickness of the adsorbed polymer and the position of the maximum in the density profile stay relatively constant with varying anchor block size. The distance between anchor points increases with increasing molecular weight of the anchor block in a manner characteristic of mushrooms. The dependence of the volume fraction of polymer at the maximum in the density profile on the mean distance between anchor groups agrees with that predicted by simple scaling arguments. A very compact surface layer of PVP is found for the polymers forming mushrooms. The polymer density profile normal to the substrate for the smallest PVP anchor block is well - described by the brush - type profile predicted by mean field theories. A crossover from mushrooms to brushes can be seen as the size of the PVP anchor block is reduced. For a more complete understanding of this system, however, measurements of the reflectivity below and above the cmc should be made.

Acknowledgments.

We are grateful to Dr. A. Rennie for his help with the D17 measurements, and Dr. H. Stanley for her help and advice at various stages of the project. Helpful discussions with Dr. R. A. L. Jones, Dr. T. Nicolai and Dr. P. van Hutten are gratefully acknowledged. JBF thanks the SERC and ICI for a CASE studentship. This work benefitted from the use of the SPEAR facility at the Manuel Lujan Jr. Neutron Scattering Center at the Los Alamos National Laboratory which is supported by the US Department of Energy, Office of Basic Energy Sciences, and other Department of Energy programs under Contract W-7405-ENG-32 to the University of California, and the use of the D17 facility at ILL, Grenoble.

References

[1] COSGROVE T., HEATH T., VAN LENT B., LEERMAKERS F., SCHEUTJENS J., *Macromolecules* **20** (1987) 1692.
[2] SATIJA S. K., MAJKRZAK C. F., RUSSELL T. P., SINHA S. K., SIROTA E. B., HUGHES G. J., *Macromolecules* **23** (1990) 3860.
[3] PENFOLD J., THOMAS R. K., *J. Phys. Condens. Matter* **2** (1990) 1369.
[4] RUSSELL T. P., *Mat. Sci. Rep.* **5** (1990).
[5] FIELD J. B., TOPRAKCIOGLU C., BALL R. C., STANLEY H. B., DAI L., BARFORD W., PENFOLD J., SMITH G., HAMILTON W., *Macromolecules* **25** (1992) 434.
[6] COSGROVE T., VINCENT B., COHEN-STUART M. A., *Adv. Colloid Interface Sci.* **24** (1986) 143.
[7] AUROY P., AUVRAY L., LEGER L., *Macromolecules* **24** (1991) 2523.
[8] MILNER S. T., WITTEN T. A., CATES M. E., *Macromolecules* **21** (1988) 2610.
[9] MILNER S. T., WITTEN T. A., CATES M. E., *Europhys. Lett.* **5** (1988) 413.
[10] SCHEUTJENS J. M. H. M., FLEER G. J., *J. Phys. Chem.* **83** (1979) 1619.
[11] SCHEUTJENS J. M. H. M., FLEER G. J., *J. Phys. Chem.* **84** (1980) 178.
[12] SCHEUTJENS J. M. H. M., FLEER G. J., *J. Adv. Colloid Interface Sci.* **16** (1982) 341.
[13] CLARK A. T., LAL M., *J. Chem. Soc., Faraday Trans. 2* **74** (1978) 1857.
[14] CHAKRABARTI A., TORAL P., *Macromolecules* **23** (1990) 2016.
[15] TAUNTON H. J., TOPRAKCIOGLU C., FETTERS L. J., KLEIN J., *Macromolecules* **23** (1990) 571.
[16] ALEXANDER S., *J. Phys. France* **38** (1977) 983.
[17] DE GENNES P. G., *J. Phys. France* **37** (1976) 1445.
[18] HADZIIOANNOU G., PATEL S., GRANICK S., TIRRELL M., *J. Am. Chem. Soc.* **108** (1986) 2869.
[19] MUNCH M. R., GAST A. P., *Macromolecules* **21** (1988) 1366.
[20] MARQUES C., JOANNY J. F., *Macromolecules* **21** (1988) 1051.

[21] MUNCH M. R., GAST A. P., *Macromolecules* **23** (1990) 2313.
[22] MUNCH M. R., GAST A. P., *J. Chem. Soc. Faraday Trans.* **86** (1990) 1341.
[23] DE GENNES P. G., *Macromolecules* **13** (1980) 1069.
[24] SHIM D. F. K., CATES M. E., *J. Phys. France* **50** (1989) 3535.
[25] PARSONAGE E., TIRRELL M., WATANABE H., NUZZO R. G., *Macromolecules* **24** (1991) 1987.
[26] OU-YANG H. D., GAO Z., *J. Phys. France* **1** (1991) 1375.
[27] MOTSCHMANN H., STAMM M., TOPRAKCIOGLU C., *Macromolecules* **24** (1991) 3681.
[28] EVERS O. A., SCHEUTJENS J. M. H. M., FLEER G. J., *J. Chem. Soc. Faraday Trans.* **86** (1990) 1333.